

# Transition between soft physics at LHC and low- $x$ physics at HERA

A.A. Grinyuk<sup>1</sup>, A.V. Lipatov<sup>2</sup>, G.I. Lykasov<sup>1</sup>, N.P. Zotov<sup>2</sup>

September 1, 2018

<sup>1</sup>*Joint Institute for Nuclear Research, Dubna 141980, Moscow region, Russia*

<sup>2</sup>*Skobeltsyn Institute of Nuclear Physics, Lomonosov Moscow State University, Moscow 119991, Russia*

## Abstract

We find out the connection between the unintegrated gluon distribution at low intrinsic transverse momenta and the inclusive spectrum of the hadrons produced in  $pp$  collision at LHC energies in the mid-rapidity region and low hadron transverse momenta. The parameters of this distribution are found from the best description of the LHC data. Its application to the analysis of  $ep$  deep inelastic scattering allows us to obtain the results which describe reasonably well the H1 and ZEUS data on the structure functions at low  $x$ . A connection between the soft processes at LHC and small  $x$  physics at HERA has been found.

PACS number(s): 12.38.-t, 13.85.-t

## 1 Introduction

Hard processes involving incoming protons, such as deep-inelastic lepton-proton scattering (DIS), are described using the scale-dependent parton density functions. Usually, these quantities are calculated as a function of the Bjorken variable  $x$  and the square of the four-momentum transfer  $q^2 = -Q^2$  within the framework of the DGLAP evolution equations [1] based on the standard collinear QCD factorization. However, for semi-inclusive processes (such as inclusive jet production in DIS, electroweak boson production [2], etc.) at high energies which are sensitive to the details of the parton kinematics it is more appropriate to use the parton distributions unintegrated over the transverse momentum  $k_t$  or, transverse momentum depend (TMD) distributions, in the framework of the  $k_t$ -factorization

QCD approach<sup>1</sup> [3]. The  $k_t$ -factorization formalism is based on the BFKL [5] or CCFM [6] evolution equations and provides a solid theoretical ground for the effects of initial gluon radiation. The unintegrated gluon  $g(x, k_t)$  (u.g.d.) and quark  $q(x, k_t)$  distributions (u.q.d.) are widely discussed and applied in phenomenological calculations in the framework of the  $k_t$ -factorization QCD approach and can be found, for example, in [7–23]<sup>2</sup>. In [2, 10] the unintegrated parton distributions (u.p.d.) were obtained using the so-called KMR prescription within the leading order (LO) and next-to-leading order of QCD (NLO) at large  $Q^2$  from the known (DGLAP-evolved [1]) parton densities determined from the global data analysis. These u.p.d. were successfully applied to analyze the DIS data at low  $x$  and a number of processes studied at the Tevatron and LHC (see, for example, [14–22]). However, at small values of  $Q^2$  the nonperturbative effects should be included to evaluate these distributions. The nonperturbative effects can arise from the complex structure of the QCD vacuum. For example, within the instanton approach the very fast increase of the unintegrated gluon distribution function at  $0 \leq k_t \leq 0.5 \text{ GeV}/c$  and  $Q^2 = 1 \text{ (GeV}/c)^2$  is obtained [11]. These results stimulated us to assume, that the u.g.d. in the proton can be determined also in the soft hadron production in  $pp$  collisions.

In this paper we analyze inclusive spectra of the hadrons produced in  $pp$  collisions at LHC energies in the mid-rapidity region in a context including the possible creation of soft gluons in the proton. We estimate the u.g.d. function at low intrinsic transverse momenta  $k_t \leq 1.5 - 1.6 \text{ GeV}/c$  and extract its parameters from the best description of the LHC data at low transverse momenta  $p_t$  of the produced hadrons. We also show that our u.g.d. similar to the u.g.d. obtained in [8] at large  $k_t$  and different from it at low  $k_t$ . The u.g.d. is directly related to the dipole-nucleon cross section within the model proposed in [7, 8] (see also [9, 28–32]) which is saturated at low  $Q$  or large transverse distances  $r \sim 1/Q$  between quark  $q$  and antiquark  $\bar{q}$  in the  $q\bar{q}$  dipole created from the splitting of the virtual photon  $\gamma^*$  in the  $ep$  DIS. Here we find a new parametrization for this dipole-nucleon cross section, as a function of  $r$ , using the saturation behavior of the gluon density.

The paper is organized as following. In Section 2 we study the inclusive spectra of hadrons in  $pp$  collisions and obtain the *modified* u.g.d. In Section 3 we discuss the connection between the u.g.d. and the dipole cross section. In Section 4 we apply the *modified* u.g.d. to describe the HERA data of the DIS structure functions: the longitudinal ( $F_L$ ), charm ( $F_2^c$ ) and bottom ( $F_2^b$ ) structure functions (SF).

## 2 Inclusive spectra of hadrons in $pp$ collisions

### 2.1 Unintegrated gluon distributions

The u.p.d. in a proton are a subject of intensive studies, and various approaches to investigate these quantities have been proposed. At asymptotically large energies (or very small  $x$ ) the theoretically correct description is given by the BFKL evolution equation [5] where the leading  $\ln(1/x)$  contributions are taken into account in all orders. Another approach, valid for both small and large  $x$ , is given by the CCFM gluon evolution equation [6]. It introduces

---

<sup>1</sup>See, for example, reviews [4] for more information.

<sup>2</sup>The theoretical analysis of TMD was done recently in [24–27].

angular ordering of emissions to treat the gluon coherence effects correctly. In the limit of asymptotic high energies, it is almost equivalent to BFKL [5], but also similar to the DGLAP evolution for large  $x \sim 1$ . The resulting u.g.d. depends on two scales, the additional scale  $\bar{q}$  is a variable related to the maximum angle allowed in the emission and plays the role of the evolution scale  $\mu$  in the collinear parton densities. In the two-scale u.p.d. obtained from the conventional ones using the Kimber-Martin-Ryskin (KMR) prescription [2, 10], the  $k_t$  dependence in the unintegrated parton distributions enters only in the last step of evolution. Such a procedure is expected to include the main part of the collinear higher-order QCD corrections. Finally, a simple parametrization of the unintegrated gluon density was obtained within the color-dipole approach in [7, 8] on the assumption of saturation of the gluon density at low  $Q^2$  which successfully described both inclusive and diffraction  $ep$  scattering. This gluon density  $xg(x, k_t^2, Q_0^2)$  is given by [8, 9]

$$xg(x, k_t, Q_0) = \frac{3\sigma_0}{4\pi^2\alpha_s(Q_0)} R_0^2(x) k_t^2 \exp(-R_0^2(x) k_t^2), \quad R_0(x) = \frac{1}{Q_0} \left( \frac{x}{x_0} \right)^{\lambda/2}, \quad (1)$$

where  $\sigma_0 = 29.12$  mb,  $\alpha_s = 0.2$ ,  $Q_0 = 1$  GeV,  $\lambda = 0.277$  and  $x_0 = 4.1 \cdot 10^{-5}$ . This simple expression corresponds to the Gaussian form for the effective dipole cross section  $\hat{\sigma}(x, r)$  as a function of  $x$  and the relative transverse separation  $\mathbf{r}$  of the  $q\bar{q}$  pair [8]. In fact, this form can be more complicated. In this paper we study this point and try to find a parametrization for  $xg(x, k_t, Q_0)$ , which is related to  $\hat{\sigma}(x, r)$ , from the best description of the inclusive spectra of charge hadrons produced in  $pp$  collisions at LHC energies and mid-rapidity region.

## 2.2 Quark-gluon string model (QGSM) including gluons

The soft hadron production in  $pp$  collisions at not too large momentum transfer can be analyzed within the soft QCD models, namely, the quark-gluon string model (QGSM) [33–35] or the dual parton model (DPM) [36]. The cut  $n$ -pomeron graphs calculated within these models result in a reasonable description at small but nonzero rapidities. However, it has been shown recently [37, 38] that there are some difficulties in using the QGSM to analyze inclusive spectra in  $pp$  collisions in the mid-rapidity region and at the initial energies above the ISR one. However, it is due to the Abramovsky-Gribov-Kancheli cutting rules (AGK) [39] at mid-rapidity ( $y \simeq 0$ ), when only one-pomeron Mueller-Kancheli diagrams contribute to the inclusive spectrum  $\rho_h(y \simeq 0, p_t)$ . To overcome these difficulties it was assumed [37] that there are soft gluons or the so called *intrinsic* gluons in the proton suggested in [40], which split into  $q\bar{q}$  pairs and should vanish at the zero intrinsic transverse momentum ( $k_t \sim 0$ ) because at  $k_t \sim 0$  the conventional QGSM (without the *intrinsic* gluons) [33] is applied very well. The inclusive spectrum of hadrons  $E d\sigma/d^3p(y \simeq 0) \equiv \rho_h(y \simeq 0, p_t)$  was split into two parts, the quark contribution  $\rho_q(y \simeq 0, p_t)$  and the gluon one and their energy dependence was calculated in [37, 38]

$$\rho_h(y \simeq 0, p_t) = \rho_q(y \simeq 0, p_t) + \rho_g(y \simeq 0, p_t), \quad (2)$$

where  $\rho_q(y \simeq 0, p_t)$  is the quark contribution and  $\rho_g(y \simeq 0, p_t)$  is the contribution of gluons to the spectrum  $\rho_h(y \simeq 0, p_t)$ . It was shown [38] that the AGK cutting rules for the inclusive

spectrum at  $x \simeq 0$  can be proofed within the QGSM [33] and  $\rho_q(y \simeq 0, p_t)$  can be presented in the form

$$\rho_q(0, p_t) = \sum_{n=1}^{\infty} \sigma_n(s) \phi_n^q(0, p_t), \quad (3)$$

where  $\phi_n^q$  is the convolution of the quark distribution and the fragmentation function of the quark  $q$  to the hadron  $h$  that at  $x \simeq 0$  ( $y \simeq 0$ ) is proportional to the pomeron number  $n$ , see (9) and (10) in [38]. Therefore, (3) is presented in the form

$$\rho_q(0, p_t) = \tilde{\phi}_q(0, p_t) \sum_{n=1}^{\infty} n \sigma_n(s), \quad (4)$$

where  $\sigma_n$  is the cross section for production of the  $n$ -pomeron chain (or  $2n$  quark-antiquark strings) decaying into hadrons, calculated within the “eikonal approximation” [41], the function  $\tilde{\phi}_q(0, p_t)$  is related to the pomeron-hadron vertex in the Mueller-Kancheli diagram. Inserting  $\sigma_n$  into (4) the quark contribution  $\rho_q(0, p_t)$  of the spectrum is presented in the form [38]

$$\rho_q(0, p_t) = g(s/s_0)^{\Delta} \tilde{\phi}_q(0, p_t), \quad (5)$$

where  $g = 21$  mb,  $\Delta = \alpha_P(0) - 1 \simeq 0.12$ ,  $\alpha_P(0)$  is the intercept of the sub-critical Pomeron, the function  $\tilde{\phi}_q(0, p_t)$  is found from the fit of the SPS and LHC data on the inclusive spectra of charged hadrons in the mid-rapidity at the initial energies from 540 GeV till 7 TeV.

The *intrinsic* gluons split into the sea  $q\bar{q}$  pairs, therefore its contribution to the inclusive spectrum is due to the contribution of the sea quarks, which, according to the QGSM ideology [33], contribute to the  $n$ -pomeron shower at  $n \geq 2$ . Therefore, the contribution  $\rho_g(y \simeq 0, p_t)$  is presented in the form similar to (4) replacing  $\tilde{\phi}_q(0, p_t)$  by  $\tilde{\phi}_g(0, p_t)$  and inputting  $n \geq 2$

$$\begin{aligned} \rho_g(0, p_t) &= \tilde{\phi}_g(0, p_t) \sum_{n=2}^{\infty} n \sigma_n(s) \equiv \\ &\tilde{\phi}_g(0, p_t) \left( \sum_{n=1}^{\infty} n \sigma_n(s) - \sum_{n=1}^{\infty} \sigma_n(s) \right) = \\ &\tilde{\phi}_g(0, p_t) (g(s/s_0)^{\Delta} - \sigma_{nd}), \end{aligned} \quad (6)$$

where  $\sigma_{nd} = \sum_{n=1}^{\infty} \sigma_n(s)$  is the nondiffractive cross section, the function  $\tilde{\phi}_g(0, p_t)$  is also found from the fit of the SPS and LHC data on the inclusive spectra of charged hadrons in the mid-rapidity region [38]. The following parametrizations for  $\tilde{\phi}_q(0, p_t)$  and  $\tilde{\phi}_g(0, p_t)$  were found [37]:

$$\begin{aligned} \tilde{\phi}_q(0, p_t) &= A_q \exp(-b_q p_t), \\ \tilde{\phi}_g(0, p_t) &= A_g \sqrt{p_t} \exp(-b_g p_t), \end{aligned} \quad (7)$$

where  $s_0 = 1$  GeV $^2$ ,  $g = 21$  mb,  $\Delta = 0.12$ . The parameters are fixed [37] from the fit to the data on the  $p_t$  distribution of charged particles at  $y = 0$ :  $A_q = 4.78 \pm 0.16$  (GeV/c) $^{-2}$ ,  $b_q = 7.24 \pm 0.11$  (GeV/c) $^{-1}$  and  $A_g = 1.42 \pm 0.05$  (GeV/c) $^{-2}$ ;  $b_g = 3.46 \pm 0.02$  (GeV/c) $^{-1}$ . In Fig. 1

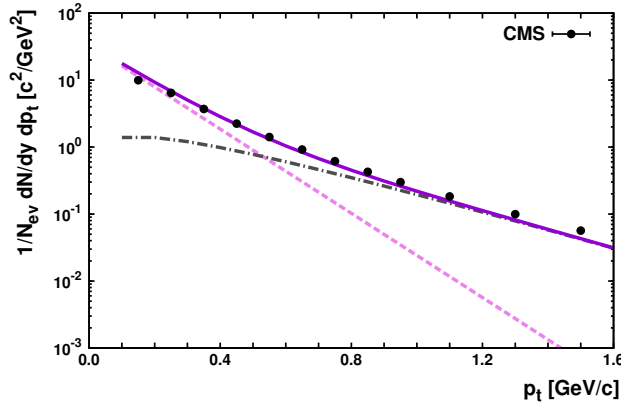


Figure 1: The inclusive spectrum of the charged hadron as a function of  $p_t$  (GeV/c) in the central rapidity region ( $y = 0$ ) at  $\sqrt{s} = 7$  TeV at  $p_t \leq 1.6$  GeV/c compared with the CMS measurements [42] which are very close to the ATLAS data [43]. The dashed and dash-dotted curves correspond to the quark and gluon contribution given by (5) and (6), respectively. The solid curve represents their sum.

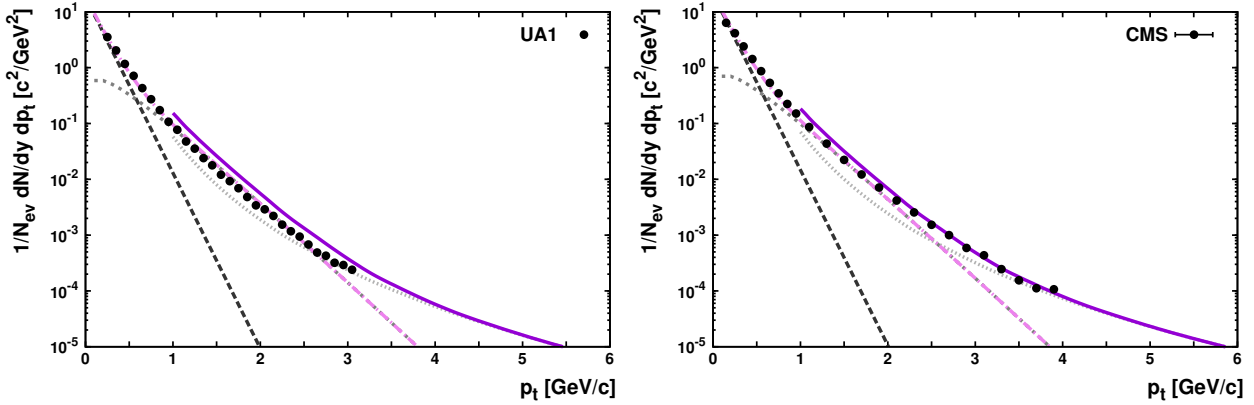


Figure 2: The inclusive spectrum of charged hadron as a function of  $p_t$  (GeV/c) in the central rapidity region ( $y = 0$ ) at  $\sqrt{s} = 540$  GeV (left) and  $\sqrt{s} = 900$  GeV (right) compared with the UA1 [44] and CMS [42] data. The long dashed curves are the quark contribution  $\rho_q(x = 0, p_t)$  (5), the short dashed curves correspond to the gluon one  $\rho_g(x = 0, p_t)$  (6), the dash-dotted curves are the sum of the quark and gluon contributions (2), the dotted curves correspond to the perturbative LO QCD [38]. The solid curves represent the sum of the calculations within the soft QCD including the gluon contribution (2) and the perturbative LO QCD.

we illustrate the fit of the inclusive spectrum of charged hadrons produced in  $pp$  collisions at  $\sqrt{s} = 7$  TeV and the central rapidity region at the hadron transverse momenta  $p_t \leq 1.6$  GeV/c. Here the solid line corresponds to the quark contribution  $\rho_q$ , the dashed line is the gluon contribution  $\rho_g$ , and the dotted curve is the sum of these contributions  $\rho_h$  given by

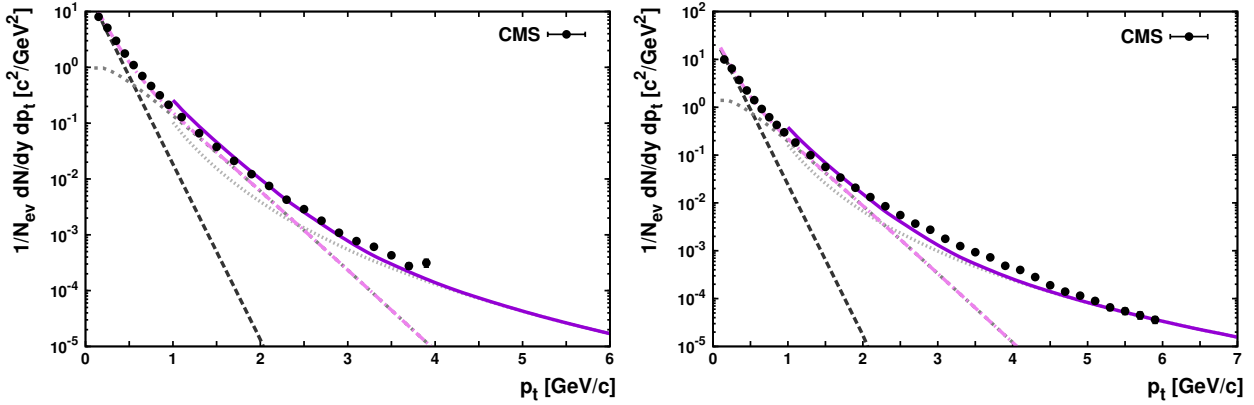


Figure 3: The inclusive spectrum of charged hadron as a function of  $p_t$  (GeV/c) in the central rapidity region ( $y = 0$ ) at  $\sqrt{s} = 2.36$  TeV (left) and  $\sqrt{s} = 7$  TeV (right) compared with the CMS [42] and ATLAS [43] data. Notation of all curves is the same as in Fig. 2.

(2). The little discrepancy between the data and our calculation (the dotted line) at  $p_t > 1.2$  GeV/c disappears if the contribution of the perturbative QCD within the LO is included. It is shown in Figs. 2 and 3, where the inclusive hadron spectrum is presented at  $\sqrt{s} = 0.54$ , 0.9, 2.36 and 7 TeV, where the dash-dotted line is the sum of the spectrum  $\rho_h(x = 0, p_t)$  (2) and the short dash-dotted line is the result of calculation within the LO PQCD [38]. The quite satisfactory description of the data on such spectra was obtained in [38] at the SPS and LHC energies using (2) for  $\rho_h(x = 0, p_t)$  and the LO PQCD calculations both together. Therefore we conclude that the energy dependence of the inclusive spectrum of charged hadrons produced in the  $pp$  collision at the mid-rapidity region is reasonably well described using the parametrization (7) for  $\tilde{\phi}_q(0, p_t)$  and  $\tilde{\phi}_g(0, p_t)$ .

### 2.3 Modified unintegrated gluon distributions

As it can be seen in Figs. 1 — 3 the contribution to the inclusive spectrum at  $y \simeq 0$  due to the *intrinsic* gluons is sizable at low  $p_t < 2$  GeV/c, e.g., in the soft kinematical region. Therefore, we can estimate this contribution within the nonperturbative QCD model, similar to the QGSM [33]. We calculate the gluon contribution  $\tilde{\phi}_g(x \simeq 0, p_t)$  entering into (6) as the cut graph (Fig. 4, right) of the one-pomeron exchange in the gluon-gluon interaction (Fig. 4, left) using the splitting of the gluons into the  $q\bar{q}$  pair. The right diagram of Fig. 4 corresponds to the creation of two colorless strings between the quark/antiquark ( $q/\bar{q}$ ) and antiquark/quark ( $\bar{q}/q$ ). Then, after their brake,  $q\bar{q}$  are produced and fragmented into the hadron  $h$ . Actually, the calculation can be made in a way similar to the calculation of the sea quark contribution to the inclusive spectrum within the QGSM [33], e.g., the contribution  $\tilde{\phi}_g(0, p_t)$  is presented as the sum of two convolution functions

$$\tilde{\phi}_g(x, p_t) = F_q(x_+, p_{ht})F_{\bar{q}}(x_-, p_{ht}) + F_{\bar{q}}(x_+, p_{ht})F_q(x_-, p_{ht}), \quad (8)$$

where the function  $F_{q(\bar{q})}(x_+, p_{ht})$  corresponds to the production of the hadron  $h$  from the decay of the upper vertex of  $q\bar{q}$  string and  $F_{q(\bar{q})}(x_-, p_{ht})$  corresponds to the production of

$h$  from the decay of the bottom vertex of  $q\bar{q}$  string. They are calculated as the following convolution:

$$F_{q(\bar{q})}(x_{\pm}, p_{ht}) = \int_{x_{\pm}}^1 dx_1 \int d^2 k_{1t} f_{q(\bar{q})}(x_1, k_{1t}) G_{q(\bar{q}) \rightarrow h} \left( \frac{x_{\pm}}{x_1}, p_{ht} - k_{1t} \right). \quad (9)$$

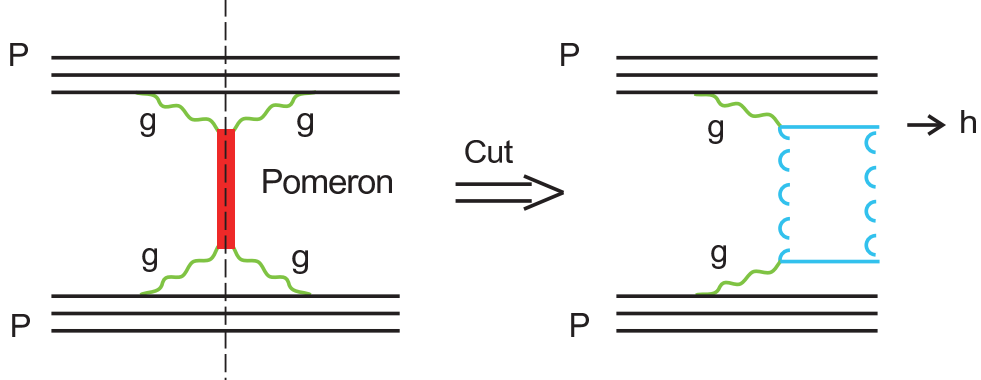


Figure 4: The one-pomeron exchange graph between two gluons in the elastic  $pp$  scattering (left) and the cut one-pomeron due to the creation of two colorless strings between quarks/antiquarks that decay into  $q\bar{q}$  pairs, which are drawn as the semi-circles (right) [33].

Here  $G_{q(\bar{q}) \rightarrow h}(z, \tilde{k}_t) = z D_{q(\bar{q}) \rightarrow h}(z, \tilde{k}_t)$ ,  $D_{q(\bar{q}) \rightarrow h}(z, \tilde{k}_t)$  is the fragmentation function (FF) of the quark (antiquark) to the hadron  $h$ ,  $z = x_{\pm}/x_1$ ,  $\tilde{k}_t = p_{ht} - k_t$ ,  $x_{\pm} = 0.5(\sqrt{x^2 + x_t^2} \pm x)$ ,  $x_t = 2\sqrt{(m_h^2 + p_t^2)/s}$ . At  $x \simeq 0$ , we get that  $x_+$  and  $x_-$  are equivalent to each other, e.g.,  $x_+ = x_- = m_t/\sqrt{s}$ . The distribution of sea quarks (antiquark)  $f_{q(\bar{q})}$  is related to the splitting function  $\mathcal{P}_{g \rightarrow q\bar{q}}$  of gluons to  $q\bar{q}$  by

$$f_{q(\bar{q})}(z, k_t) = \int_z^1 g(z_1, k_t, Q_0) \mathcal{P}_{g \rightarrow q\bar{q}} \left( \frac{z}{z_1} \right) \frac{dz_1}{z_1}, \quad (10)$$

where  $g(z_1, k_{1t}, Q_0)$  is the u.g.d. The gluon splitting function  $\mathcal{P}_{g \rightarrow q\bar{q}}$  was calculated within the Born approximation. In (10) we assumed the collinear splitting of the *intrinsic* gluon to the  $q\bar{q}$  pair because values of  $k_t$  are not zero but small.

Calculating the diagram of Fig. 4 (right) by the use of (8) — (10) for the gluon contribution  $\rho_g$  we took the FF to charged hadrons, pions, kaons, and  $p\bar{p}$  pairs obtained within the QGSM [46]. From the best description of  $\rho_g(x \simeq 0, p_{ht})$ , see its parametrization given by (7), we found the form for the  $xg(x, k_t, Q_0)$  which was fitted in the following way:

$$xg(x, k_t, Q_0) = \frac{3\sigma_0}{4\pi^2 \alpha_s(Q_0)} C_1 (1-x)^{b_g} \times \left( R_0^2(x) k_t^2 + C_2 (R_0(x) k_t)^a \right) \exp \left[ -R_0(x) k_t - d(R_0(x) k_t)^3 \right], \quad (11)$$

where  $R_0(x)$  is defined in (1). The coefficient  $C_1$  was found from the following normalization:

$$g(x, Q_0^2) = \int_0^{Q_0^2} dk_t^2 g(x, k_t^2, Q_0^2), \quad (12)$$

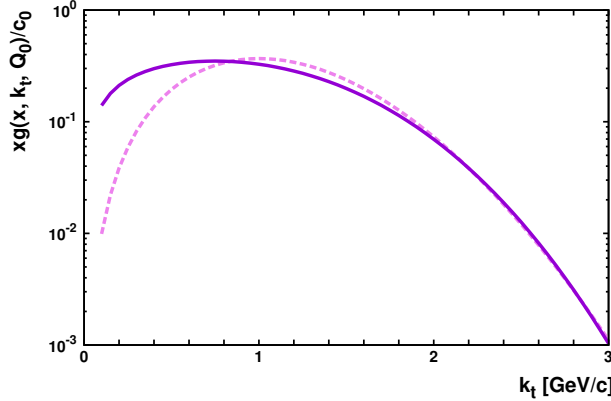


Figure 5: The unintegrated gluon distribution  $xg(x, k_t, Q_0)/c_0$  (where  $c_0 = 3\sigma_0/(4\pi^2\alpha_s(Q_0))$ ) as a function of  $k_t$  at  $x = x_0$  and  $Q_0 = 1$  GeV/c. The solid and dashed curves correspond to the modified u.g.d. (11) and original GBW gluon density [7] given by (1), respectively.

and the parameters  $a = 0.7$ ,  $C_2 \simeq 2.3$ ,  $\lambda = 0.22$ ,  $b_g = 12$ ,  $d = 0.2$ ,  $C_3 = 0.3295$  were found from the best fit of the LHC data on the inclusive spectrum of charged hadrons produced in  $pp$  collisions and in the mid-rapidity region as it can be seen in Figs. 1 — 3.

In Fig. 5 we present the modified u.g.d. obtained by calculating the cut one-pomeron graph of Fig. 4 and the original GBW u.g.d. [7] as a function of the transverse gluon momentum  $k_t$ . One can see that the modified u.g.d. (the solid line in Fig. 5) is different from the original GBW gluon density [7] at small  $k_t < 1.5$  GeV/c and coincides with it at larger  $k_t$ . This is due to the sizeable contribution of  $\rho_g$  in (6) and (7) to the inclusive spectrum  $\rho(p_t)$  of charged hadrons produced in  $pp$  collisions at LHC energies and in the mid-rapidity region (see the dashed line in Fig. 1).

Let us also note that, as it was shown recently in [45], the modified GBW given by (11) describes reasonably well the HERA data on the proton longitudinal structure function  $F_L(Q^2)$  at low  $x$ .

### 3 Saturation dynamics

According to [7, 8] (see also [29–31]), the u.g.d. can be related to the cross section  $\hat{\sigma}(x, r)$  of the  $q\bar{q}$  dipole with the nucleon. This dipole is created from the split of the virtual exchanged photon  $\gamma^*$  to  $q\bar{q}$  pair in  $ep$  deep inelastic scattering (DIS). The relation at the fixed  $Q_0^2$  is the following [8]:

$$\hat{\sigma}(x, r) = \frac{4\pi\alpha_s(Q_0^2)}{3} \int \frac{d^2 k_t}{k_t^2} \{1 - J_0(r k_t)\} xg(x, k_t). \quad (13)$$

Using the simple form for  $xg(x, k_t)$  given by (1) as input to (13) one can get the following

form for the dipole cross section:

$$\hat{\sigma}_{\text{GBW}}(x, r) = \sigma_0 \left\{ 1 - \exp \left( -\frac{r^2}{4R_0^2(x)} \right) \right\}. \quad (14)$$

However, the modified u.g.d. given by (11) inputted to (13) results in a more complicated form for  $\hat{\sigma}(x, r)$ :

$$\hat{\sigma}_{\text{modif}}(x, r) = \sigma_0 \left\{ 1 - \exp \left( -\frac{b_1 r}{R_0(x)} - \frac{b_2 r^2}{R_0^2(x)} \right) \right\}, \quad (15)$$

where  $b_1 = 0.045$  and  $b_2 = 0.3$ . In Fig. 6 we show the difference between the dipole cross section  $\hat{\sigma}_{\text{GBW}}(x = x_0, r)$  [8] and  $\hat{\sigma}_{\text{modif}}(x = x_0, r)$  obtained from the modified u.g.d. given by (11). The saturation effect means that the dipole cross section becomes constant when  $r > 2R_0$ . As it was shown in [7, 8], at low  $Q^2$  the transverse  $\gamma^* p$  cross section calculated within the dipole model is about constant when  $QR_0 < 1$ . It means that  $Q_s \sim 1/R_0$  can be treated as the saturation scale. One can see in Fig. 6 that the modified dipole cross section is saturated a little earlier than the GBW one.

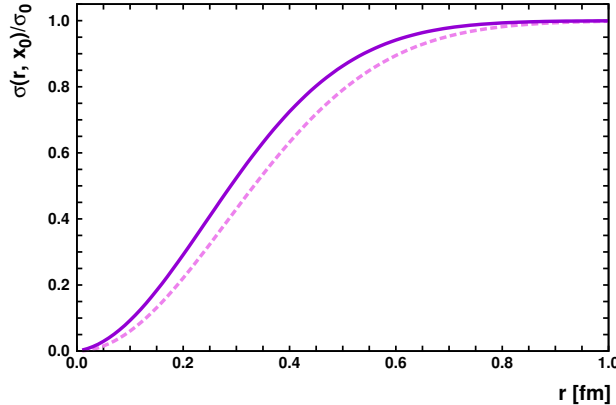


Figure 6: The dipole cross section  $\hat{\sigma}/\sigma_0$  at  $x = x_0$  as a function of  $r$ . The solid and dashed curves correspond to our calculations and calculation of [8], respectively.

There are different forms of the dipole cross sections suggested in [28–30, 48]. The dipole cross section can be presented in the general form [7]:

$$\hat{\sigma}(x, r) = \sigma_0 g(\hat{r}^2), \quad (16)$$

where  $\hat{r} = r/(2R_0(x))$ . The function  $g(\hat{r}^2)$  can be written in the form [28]

$$g(\hat{r}^2) = \hat{r}^2 \log \left( 1 + \frac{1}{\hat{r}^2} \right), \quad (17)$$

or in the form [48]

$$g(\hat{r}^2) = 1 - \exp \left\{ -\hat{r}^2 \log \left( \frac{1}{\Lambda r} + e \right) \right\}, \quad (18)$$

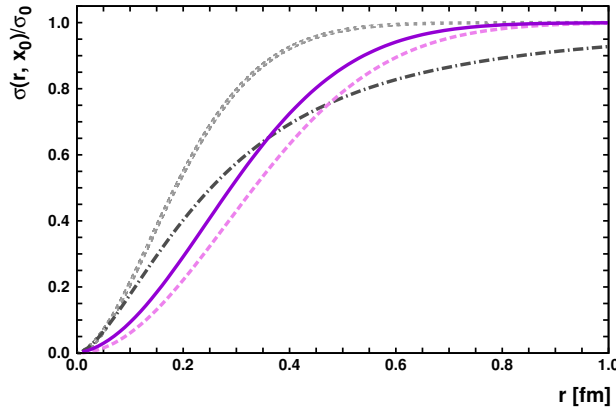


Figure 7: The dipole cross section  $\hat{\sigma}/\sigma_0$  at  $x = x_0$  as a function of  $r$ . The solid, dashed, dash-dotted and dotted curves correspond to our calculations, calculations of [8], calculations of [28] and [48], respectively.

where saturation occurs for larger  $r$ . In Fig. 7 we illustrate the dipole cross sections  $\hat{\sigma}/\sigma_0$  at  $x = x_0$  which are saturated at  $r > 0.6$  fm, obtained in [28, 47, 48]. They are compared with the results of our calculations (solid line) given by (15). The solid curve in Fig. 7 corresponds to the modified u.g.d. given by (11), which allowed us to describe the LHC data on inclusive spectra of hadrons produced in the mid-rapidity region of  $pp$  collision at low  $p_t$ . Therefore, the form of the dipole-nucleon cross sections presented in Fig. 7 can be verified by the description of the last LHC data on hadron spectra in soft kinematical region.

Comparing the solid curve ("Modified  $\sigma$ ") and dashed curve ("GBW  $\sigma$ ") in Fig. 7 one can see that  $\hat{\sigma}_{\text{modif}}(x, r)$  given by (15) is saturated earlier than  $\hat{\sigma}_{\text{GBW}}(x, r)$  given by (14) with increasing the transverse dimension  $r$  of the  $q\bar{q}$  dipole. If  $R_0 = (1/\text{GeV}) (x/x_0)^{\lambda/2}$ , according to [7, 8], then the saturation scale has the form  $Q_s \sim 1/R_0 = Q_{s0}(x_0/x)^{\lambda/2}$ , where  $Q_{s0} = 1 \text{ GeV} = 0.2 \text{ fm}^{-1}$ . The saturation of the dipole cross section (14) sets in when  $r \sim 2R_0$  or  $Q_s \sim (Q_{s0}/2)(x_0/x)^{\lambda/2}$ . Comparing the saturation properties of the modified  $\sigma$  and GBW  $\sigma$  presented in Fig. 7 one can get slightly larger value for  $Q_{s0}$  in comparison with  $Q_{s0} = 1 \text{ GeV}$ .

## 4 Proton structure functions

The basic information on the internal structure of the proton can be extracted from the process of deep inelastic  $ep$  scattering. Its differential cross-section has the form:

$$\frac{d^2\sigma}{dxdy} = \frac{2\pi\alpha_{em}^2}{xQ^4} \left[ \left(1 - y + \frac{y^2}{2}\right) F_2(x, Q^2) - \frac{y^2}{2} F_L(x, Q^2) \right], \quad (19)$$

where  $F_2(x, Q^2)$  and  $F_L(x, Q^2)$  are the transverse and longitudinal proton structure functions,  $x = Q^2/2(p \cdot q)$  and  $y = Q^2/xs$  are the usual Bjorken variables with  $p$ ,  $q$  and  $s$  being the proton and photon four-momenta and total  $ep$  center-of-mass energy, respectively. In

the present paper we will concentrate on the charm and beauty part of  $F_2(x, Q^2)$  and on the longitudinal SF  $F_L(x, Q^2)$ . Theoretical analysis [52–57] have generally confirmed that  $F_2^c(x, Q^2)$  and  $F_2^b(x, Q^2)$  data can be described through perturbative generation of charm and beauty within QCD. The longitudinal SF  $F_L(x, Q^2)$  is very sensitive to QCD processes since it is directly connected to the gluon content of the proton. It is equal to zero in the parton model with spin 1/2 partons and has nonzero values in the framework of pQCD.

In the  $k_t$ -factorization approach [3], the study of charm and beauty contributions to the proton SF  $F_2(x, Q^2)$  and longitudinal SF  $F_L(x, Q^2)$  has been performed previously in [14–16]. In these calculations the different approaches to evaluate the unintegrated gluon density in a proton have been tested and a reasonable well agreement with the HERA data has been found, in particular, with the CCFM-evolved gluon density proposed in [9]. Below we apply the unintegrated gluon distribution given by (7) to describe recent experimental data [49, 50, 58–62] on  $F_2^c(x, Q^2)$ ,  $F_2^b(x, Q^2)$  and  $F_L(x, Q^2)$  taken by the H1 and ZEUS collaborations at HERA. The main formulas have been obtained previously in [14]. Here we only recall some of them.

According to the  $k_t$ -factorization prescription, the considered proton SF can be calculated as a following double convolution:

$$F_2^{c,b}(x, Q^2) = \int \frac{dy}{y} \int dk_t^2 \mathcal{C}_2(x/y, k_t^2, Q^2, \mu^2) f_g(y, k_t^2, \mu^2), \quad (20)$$

$$F_L(x, Q^2) = \sum_f e_f^2 \int \frac{dy}{y} \int dk_t^2 \mathcal{C}_L(x/y, k_t^2, Q^2, \mu^2) f_g(y, k_t^2, \mu^2), \quad (21)$$

where  $e_f^2$  is the electric charge of the quark of flavor  $f$ . The hard coefficient functions  $\mathcal{C}_{2,L}(x, k_t^2, Q^2, \mu^2)$  correspond to the quark-box diagram for the photon-gluon fusion subprocess and have been calculated in [14]. Numerically, here we set charm and beauty quark masses to  $m_c = 1.4$  GeV and  $m_b = 4.75$  GeV and use the LO formula for the strong coupling constant  $\alpha_s(\mu^2)$  with  $n_f = 4$  quark flavours at  $\Lambda_{\text{QCD}} = 200$  MeV, such that  $\alpha_s(M_Z^2) = 0.1232$ . Note that in order to take into account the NLO corrections (which are important at low  $Q^2$ ) in our numerical calculations we apply the method proposed in [51]. Following [16, 51], we use the shifted value of the renormalization scale  $\mu_R^2 = K Q^2$ , where  $K = 127$ . As is was shown in [51], this shifted scale in the DGLAP approach at LO approximation leads to the results which are very close to the NLO ones. In the case of  $k_t$ -factorization this procedure gives us a possibility to take into account additional higher-twist and non-logarithmic NLO corrections [16].

The results of our calculations are presented in Figs. 8–10 in comparison with recent H1 and ZEUS data [49, 50, 58–62]. Note that the data [49, 50] on the longitudinal SF  $F_L(x, Q^2)$  refer to the fixed value of the hadronic mass  $W = 276$  GeV. The solid and dashed curves correspond to the results obtained using the modified u.g.d. (7) and the original GBW gluon, respectively. One can see that the predictions obtained with the u.g.d. (7) are in a reasonable agreement with the available HERA data for  $F_2^{c,b}(x, Q^2)$  as well as for longitudinal SF  $F_L(x, Q^2)$ . Moreover, the shape of measured SF at moderate and large  $x$  values at high  $Q^2$  is better reproduced by the modified u.g.d. (7) compared to the original GBW one. When  $x$  becomes small, the predictions of both gluon distributions under consideration practically

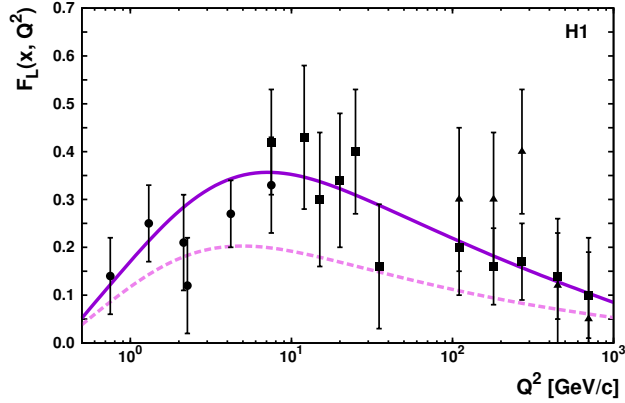


Figure 8: The longitudinal structure function  $F_L(x, Q^2)$  at fixed  $W = 276$  GeV and  $\mu_R^2 = K \cdot Q^2$ , where  $K = 127$  [51]. Notation of all curves is the same as in Fig. 5. The H1 data are taken from [49, 50].

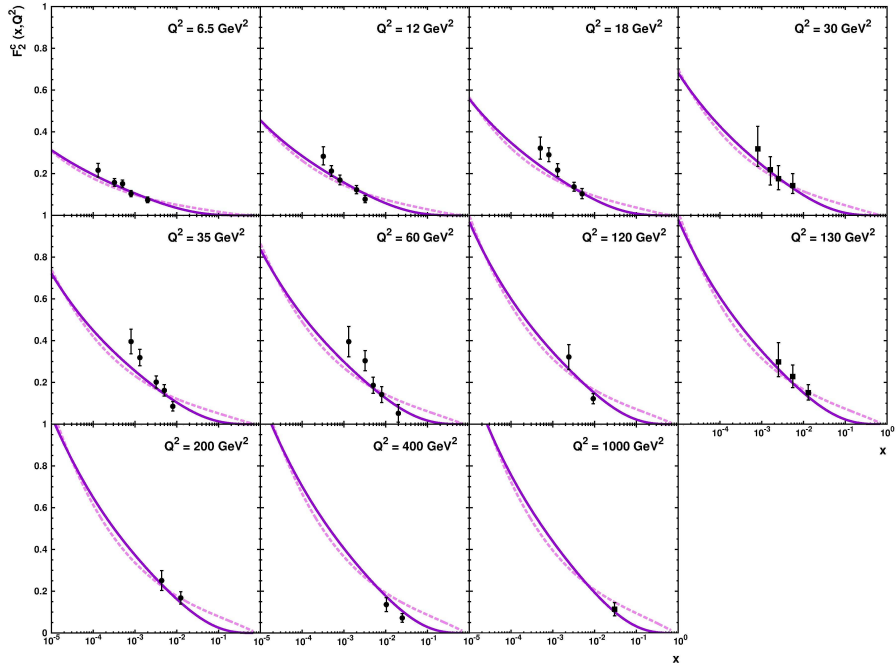


Figure 9: The charm structure function  $F_{2c}(x, Q^2)$ . Notation of all curves is the same as in Fig. 5. The data are taken from [58–60, 62].

coincide. Therefore we conclude that the link between soft processes at the LHC and low- $x$  physics at HERA is found, when we use the modified u.g.d. obtained from the description of  $pp$ -spectra at the LHC for the analyses of the behaviour of proton structure functions

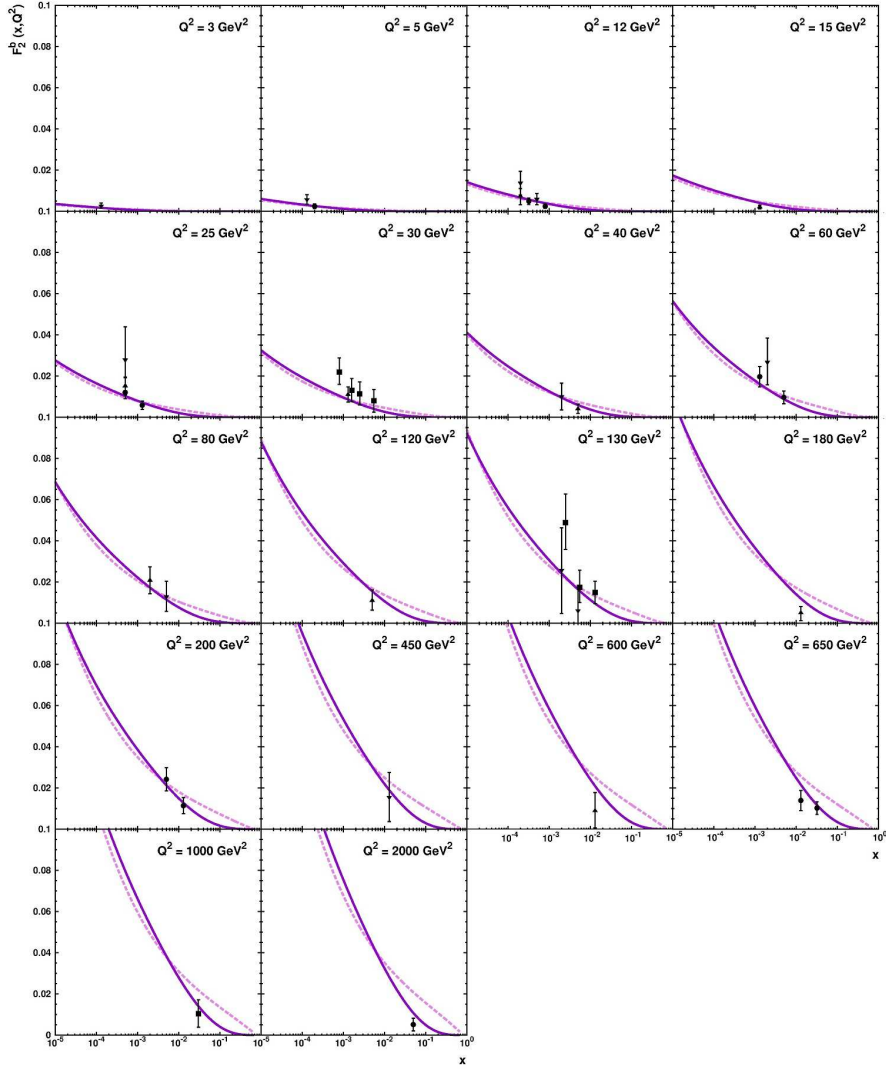


Figure 10: The bottom structure function  $F_{2b}(x, Q^2)$ . Notation of all curves is the same as in Fig. 5. The data are taken from [58, 59, 61, 62].

at HERA. Of course, it will be important for further studies of small- $x$  physics at hadron colliders.

## 5 Conclusion

We have fitted experimental data on the inclusive spectra of charged particles produced in the central  $pp$  collisions at high energies taking into account the sum of the quark  $\rho_q$  and the gluon contributions  $\rho_g$  in (2) and (7). The parameters of this fit do not depend on the initial energy in wide energy interval. Assuming creation of soft gluons in the proton at low transverse momenta  $k_t$  and calculating the cut one-pomeron graph between two gluons in

colliding protons we found a form for the unintegrated gluon distribution (modified u.g.d.) as a function of  $x$  and  $k_t$  at fixed value of  $Q_0^2$ . The parameters of this u.g.d. were found from the best description of the LHC data on inclusive spectra of charged hadrons produced in the mid-rapidity  $pp$  collisions at low  $p_t$ . It was shown that the modified u.g.d. is different from the original GBW u.g.d. obtained in [8] at  $k_t \leq 1.6$  GeV/c and it coincides with the GBW u.g.d. at  $k_t > 1.6$  GeV/c.

Using the modified u.g.d. we have calculated the  $q\bar{q}$  dipole-nucleon cross section  $\hat{\sigma}_{\text{modif}}$  as a function of the transverse distance  $r$  between  $q$  and  $\bar{q}$  in the dipole and have found that it saturates faster than  $\hat{\sigma}_{\text{GBW}}$  obtained within the GBW dipole model [7,8]. Moreover, we have shown that the relation of the modified u.g.d. and  $\hat{\sigma}_{\text{modif}}$  supports the form of the dipole-nucleon cross section and the property of saturation of the gluon density.

It has been shown that the modified u.g.d. results in a reasonable description of the longitudinal structure function  $F_L(Q^2)$  at the fixed hadronic mass  $W$ . The calculations of the charm  $F_2^c(x, Q^2)$  and the bottom  $F_2^b(x, Q^2)$  structure functions, within the  $k_t$ -factorisation, with using the modified u.g.d. and the GBW u.g.d. show a not large difference between the results for  $F_2^c(x, Q^2)$  in the whole region of  $x$  and  $Q^2$  and some difference for  $F_2^b(x, Q^2)$  at low  $x$  and large  $Q^2$ . The use of the modified u.g.d. results in a better description of the HERA data at large  $Q^2$  and small  $x$ . Therefore the link between soft processes at the LHC and low- $x$  physics at HERA has been found, since the modification of the u.g.d. leads to a satisfactory description of both the LHC and HERA data.

## 6 Acknowledgments

We thank H. Jung for extremely helpful discussions and recommendations in the preparation of this paper. The authors are grateful to S.P. Baranov, J. Bartels, B.I. Ermolaev, A.V. Kotikov, E.A. Kuraev, L.N. Lipatov, E. Levin, M. Mangano, C. Merino, M.G. Ryskin, Yu.M. Shabelskiy for useful discussions and comments. A.V.L. and N.P.Z. are very grateful to the DESY Directorate for the support within the Moscow — DESY project on Monte-Carlo implementation for HERA — LHC. This research was also supported by the FASI of the Russian Federation (grant NS-3920.2012.2), FASI state contract 02.740.11.0244 and RFBR grants 11-02-01454-a, 11-02-01538-a and 12-02-31030.

## References

- [1] V.N. Gribov and L.N. Lipatov, Sov.J. Nucl. Phys. **15** (1972) 438; G. Altarelli, G. Parisi, Nucl. Phys. B **126** (1997) 298; Yu.L. Dokshitzer, Sov. Phys. JETP, **46** (1977) 641.
- [2] M.A. Kimber, A.D. Martin, M.G. Ryskin, Phys. Rev. D **63** (2001) 114027; G. Watt, A.D. Martin, M.G. Ryskin, Eur. Phys. J. C **31** (2003) 73 [arXiv:hep-ph/0306169];
- [3] L.V. Gribov, E.M. Levin, M.G. Ryskin, Phys. Rep. **100** (1983) 1; E.M. Levin, M.G. Ryskin, Yu.M. Shabelsky, A.G. Shuvaev, Sov. J. Nucl. Phys. **53** (1991) 657;

S. Catani, M. Ciafoloni, F. Hautmann, Nucl. Phys. B **366** (1991) 135;  
 J.C. Collins, R.K. Ellis, Nucl. Phys. B **360** (1991) 3.

[4] Bo Andersson., *et.al.* (Small- $x$  Collaboration), Eur.Phys.J. C**25** (2002) 77;  
 J. Andersen *et al.* (Small- $x$  Collaboration), Eur. Phys. J. C **35** (2004) 67;  
 J. Andersen *et al.* (Small- $x$  Collaboration), Eur. Phys. J. C **48** (2006) 53.

[5] L.N. Lipatov, Sov. J. Nucl. Phys., **23** (1976) 338; E.A. Kuraev, L.N. Lipatov, V.S. Fadin, Sov. Phys. JETP **44** (1976) 443; *ibid* **45** (1977) 199; Ya.Ya. Balitzki, L.N. Lipatov, Sov.J. Nucl. Phys. **28** (1978) 822; L.N. Lipatov, Sov. Phys. JETP **63** (1986) 904.

[6] M. Ciafaloni, Nucl. Phys. B **296** (1988) 49; C. Catani, F. Fiorani, G. Marchesini, Phys. Lett. B **234** (1990) 339; *ibid* Nucl. Phys. B **336** (1990) 18; G. Marchesini, Nucl. Phys. B **445** (1995) 49; *ibid* Phys. Rev. D **70** (2004) 014012; [Erratum-*ibid.* D **70** (2004) 079902] [arXiv:hep-ph/0309096].

[7] K. Golec-Biernat, M. Wusthoff, Phys. Rev. D **59** (1998) 014017.

[8] K. Golec-Biernat, M. Wusthoff, Phys. Rev. D **60** (1999) 114023.

[9] H. Jung, in *Proc. of the DIS'2004, Strbske' Pleso, Slovakia*, arXiv:0411287 [hep-ph].

[10] A. D. Martin, M.G. Ryskin, G. Watt, Eur. Phys. J. C **66** (2010) 163; arXiv:/0909.5529 [hep-ph].

[11] N.I. Kochelev, Phys. Lett. B **426** (1998) 149.

[12] R.D. Ball, R.K. Ellis, JHEP **05** (2001) 053; R.D. Ball, Nucl. Phys. B **796** (2008) 137;  
 S. Marzani, R.G. Ball, Nucl. Phys. B **814** (2009) 246.

[13] B.I. Ermolaev, V. Greco, S.I. Troyan, Eur. Phys. J. C **71** (2011) 1750; *ibid* arXiv:1112.1854 [hep-ph].

[14] A.V. Kotikov, A.V. Lipatov, G. Parente, N.P. Zotov, Eur. Phys. J. C **26** (2002) 51.

[15] A.V. Kotikov, A.V. Lipatov, N.P. Zotov, Eur. Phys. J. C **27** (2003) 219.

[16] A.V. Kotikov, A.V. Lipatov, N.P. Zotov, J. Exp. Theor. Phys. **101** (2005) 811;  
 arXiv:hep-ph/0503275.

[17] S.P. Baranov, A.V. Lipatov, N.P. Zotov, Phys. Rev. D **81** (2010) 094034; *ibid* **85** (2012) 014034.

[18] A.V. Lipatov, N.P. Zotov, Phys. Lett. B **704** (2011) 189.

[19] A.V. Lipatov, M.A. Malyshev, N.P. Zotov, JHEP **12** (2011) 117; *ibid* **05** (2012) 104;  
 Phys. Lett. B **699** (2011) 93.

[20] H. Jung, M. Kraemer, A.V. Lipatov, N.P. Zotov, JHEP **01** (2011) 085; Phys. Rev. D **85** (2012) 034035

- [21] N.P. Zotov, PoS QFTHEP2011 (2011) 028, arXiv:1201.4144 [hep-ph].
- [22] A. Szczurek, Plenary talk presented at International Workshop on Diffraction in High-Energy Physics (DIFFRACTION 2012), Puerto del Carmen, Spain, Sept. 10-15, 2012.
- [23] K. Kutak, K. Golec-Biernat, S. Jadach, M. Skrzypek, JHEP **02** (2012) 117.
- [24] J.C. Collins, *Foundations of perturbative QCD*, CUP 2011.
- [25] E. Avsar, arXiv:1108.1181 [hep-ph]; arXiv:1203.1916 [hep-ph]
- [26] S. Mert Aybat, T. C. Rogers, Phys. Rev. **83** (2011) 114042.
- [27] F. Hautman, M. Hentschinski, H. Jung, Nucl. Phys. B **865** (2012) 54.
- [28] N.N. Nikolaev, B.G. Zakharov, Z. Phys. C **49** (1991) 607.
- [29] I.P. Ivanov, N.N. Nikolaev, Phys. Rev. D **65** (2002) 054004.
- [30] J. Nemchik, V. Barone, M. Genovese, N. N. Nikolaev, E. Predazzi and B. G. Zakharov, Phys. Lett. B **326** (1994) 161.
- [31] B.Z. Kopeliovich, J. Raufeisen, Lect. Notes Phys. **647** (2004) 305.
- [32] G. Gotsman, E. Levin, M. Lublinsky, U. Maor, Eur. Phys. J. C **27** (2003) 411; E. Levin, Phys. Rev. D **82** (2010) 101704(R).
- [33] A.B. Kaidalov, Z. Phys. C **12** (1982) 63; Surveys High Energy Phys. **13** (1999) 265. A.B. Kaidalov, O.I. Piskunova, Z. Phys. C **30** (1986) 145; Yad. Fiz. **43** (1986) 1545.
- [34] G.I. Lykasov, M.N. Sergeenko, Z. Phys. C **56** (1992) 697; *ibid* Z. Phys. C **52** (1991) 635; *ibid* Z. Phys. C **70** (1996) 455.
- [35] V.A. Bednyakov, G.I. Lykasov, V.V. Lyubushkin, Europhys. Lett. **92** (2010) 31001; arXiv:hep-ph/1005.0559.
- [36] A. Capella, U. Sukhatme, C.J.Tan, J, Tran Thanh Van, Phys. Rev. D**36**, 109 (1987); *ibid* Adv. Ser. Direct. High Energy Phys. **2** (1988) 428.
- [37] G.I. Lykasov, V.A. Bednyakov, A.A. Grinyuk, M. Poghosyan, Nucl. Phys. B **219-220** [Proc. Suppl.] (2011) 225; arXiv:1109.1469 [hep-ph].
- [38] V.A. Bednyakov, A.A. Grinyuk, G.I. Lykasov, M. Poghosyan, Int. J. Mod. Phys. A**27** (2012) 1250042.
- [39] V. Abramovsky, V.N. Gribov, O. Kancheli, Sov. J. Nucl. Phys. **18** (1973) 308.
- [40] S. Brodsky, C. Peterson, N. Sakai, Phys. Rev. D **23** (1981) 2745.
- [41] K.A. Ter-Martirosyan, Phys. Lett. B **44** (1973) 377; Sov. J. Nucl. Phys. **44** (1986) 817.

[42] CMS Collaboration, V. Kachatryan, et al., Phys. Rev. Lett. **105** (2010) 022002; arXiv:1005.3299 [hep-ex]; CMS-QCD, CERN-PH-EP-2010-003, Feb.2010.

[43] ATLAS Collaboration, G. Aad, et al., New J. Phys. **13** (2011) 053033; arXiv:1012.5104v2 [hep-ex].

[44] UA1 Collaboration, C. Albajar, et al., Nucl. Phys. B **335** (1990) 261.

[45] A. Grinyuk, H. Jung, G. Lykasov, A.V. Lipatov, N.P. Zotov, in *Proceedings International Workshop on Multiple Partonic Interactions at the LHC*, DESY- PROC-2012-03, p.169; arXiv:1203.0939 [hep-ph].

[46] Yu.M. Shabelsky, Sov. J. Nucl. Phys. **56** (1992) 2512.

[47] L. D. McLerran, R. Venugopalan, Phys. Lett. B **424** (1998) 15; arXiv:nucl-th/9705055.

[48] J.L. Albacete, C. Marquet, Phys. Lett. B **687** (2010) 174; arXiv:1001.1378 [hep-ph]

[49] P. Newman, J. Mod. Phys. A **19** (2004) 1061, arXiv:hep-ex/0312018.

[50] E.M. Lodzińska, arXiv:hep-ex/03111180.

[51] S.J. Brodsky, V.S. Fadin, V.T. Kim, L.N. Lipatov, G.B. Pivovarov, JETP. Lett. **70** (1999) 155.

[52] M.A.G. Aivazis, F.I. Olness, W.-K. Tung, Phys. Rev. D **50** (1994) 3085; M.A.G. Aivazis, J.C. Collins, F.I. Olness, W.-K. Tung, Phys. Rev. D **50** (1994) 3102.

[53] M. Buza, et al., Nucl. Phys. B **472** (1996) 611.

[54] J.C. Collins, Phys. Rev. D **58** (1998) 094002; M. Kramer, F.I. Olness, D.E. Soper, Phys. Rev. D **62** (2000) 096007; W.-K. Tung, S. Kretzer, C. Schmidt, J. Phys. G **28** (2002) 983.

[55] R.S. Thorne, Phys. Rev. D **73** (2006) 054019; A.D. Martin, W.J. Stirling, R.S. Thorne, G. Watt, Eur. Phys. J. C **63** (2009) 189.

[56] S. Forte, E. Laenen, P. Nason, J. Rojo, Nucl. Phys. B **834** (2010) 116.

[57] R.S. Thorne, arXiv:1201.6180.

[58] H1 and ZEUS Collaborations, H. Abramowicz et al., arXiv:1211.1182 [hep-ex].

[59] H1 Collaboration, F.D. Aaron et al., arXiv:1106.1028 [hep-ex].

[60] H1 Collaboration, F.D. Aaron et al., Phys. Lett. B **686** (2010) 91.

[61] ZEUS Collaboration, H. Abramowicz et al., Eur. Phys. J. C **71** (2011) 1573.

[62] ZEUS Collaboration, H. Abramowicz et al., Eur. Phys. J. C **65** (2010) 65.